NMR Investigation of the Structure of Aluminum-Containing Nitrogen Melilite (M'_{ss})

Kok Sing Chee and Yi-Bing Cheng*

Department of Materials Engineering, Monash University, Clayton, Victoria 3168, Australia

Mark E. Smith*

CSIRO Division of Materials Science and Technology, Private Bag 33, Rosebank MDC, Clayton, Victoria 3169, Australia, and Physics Laboratory, University of Kent, Canterbury, Kent, CT2 7NR, U.K.

Received December 20, 1994. Revised Manuscript Received February 27, 1995[⊗]

Replacement of silicon and nitrogen by aluminum and oxygen, respectively, in yttrium N-melilite ($Y_2Si_3O_3N_4$) forms an extensive solid solution M'_{ss}. M'_{ss} samples formed in the yttrium system are often phase mixtures. ^{29}Si and ^{27}Al magic-angle spinning NMR spectra can consequently be complex, but combined with X-ray diffraction, resonances associated with M'_{ss} can be identified and have elucidated possible atomic arrangements in M'_{ss}. The proposed yttrium M'_{ss} structure based on NMR results consists of AlO_4 and SiO_2N_2 coordinations only, with aluminum occupying the MgO_4 sites in the analogous akermanite structure and accounts for the apparent limit of aluminum solubility in *N*-melilite.

Introduction

Nitrogen (N-)melilites are compounds of the general formula $R_2Si_3O_3N_4$ (where R = yttrium or rare-earth metal) and occur as an intermediate phase in the sintering of Si_3N_4-based ceramics. N-melilite has a tetragonal structure that is built up of an infinite linkage of corner-sharing $Si(O,N)_4$ units in tetrahedral sheets perpendicular to the [001] direction, as shown in Figure 1. Sandwiched between the sheets are Y^{3+} or Ln^{3+} ions that hold the silicon oxynitride layers together.[1] Melilite is analogous to akermanite ($Ca_2MgSi_2O_7$) (Figure 2), in which the $[MgO_4]$ tetrahedra occupy the corner and center positions of the unit cell and are joined by $[Si_2O_7]$ units; Ca^{2+} cations fill in the spaces between the tetrahedral sheets. Substitution of Al for Si with the appropriate O for N balance in N-melilite (analogous to the substitution of Al–O for Si–N bonds in silicon–aluminum–oxygen–nitrogen (sialon) ceramics) results in a solid solution M'_{ss} with composition $R_2Si_{3-x}Al_xO_{3+x}N_{4-x}$ ($0 \le x \le 1$).[2] It was suggested in earlier work[2] that the most likely sites for Al substitution in M'_{ss} were in the corner and center tetrahedra of the unit cell (i.e., occupying the $[MgO_4]$ positions in the akermanite structure) based on bond-length considerations. However, the atomic arrangement of M'_{ss} has not been completely defined, and the predicted aluminum occupation of sites has not been experimentally verified. M'_{ss} is gaining interest as a grain boundary phase for sialon ceramics[3] as it has the potential to overcome the well-documented problems of oxidation and densification associated with Al-free N-melilite.[4,5] The substitutional site preference of Al in the M'_{ss} structure is important in determining the extent of Al solubility which has a direct effect on sintering, grain boundary devitrification, and oxidation behavior of sialon ceramics.

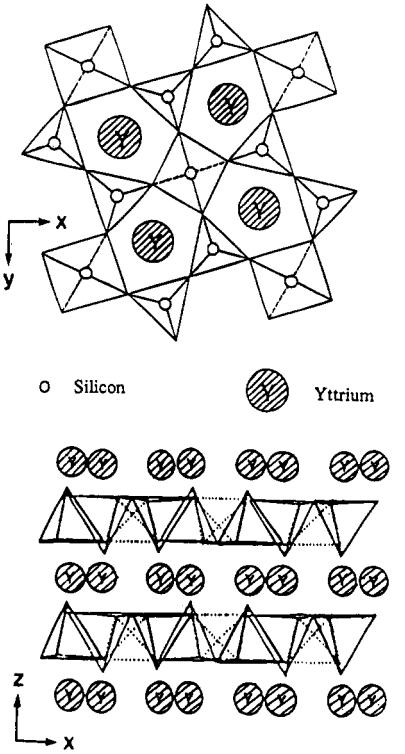

Figure 1. Structure of yttrium N-melilite (after ref 1).

^{27}Al and ^{29}Si magic-angle spinning (MAS) NMR have already provided considerable insight into the structure of different crystalline phases in sialon systems.[6,7] In

[⊗] Abstract published in *Advance ACS Abstracts,* April 1, 1995.

(1) Jack, K. H. *J. Mater. Sci.* **1976**, *11*, 1135.
(2) Cheng, Y.-B; Thompson, D. P. *J. Am. Ceram. Soc.* **1994**, *77*, 143.
(3) Cheng, Y.-B.; Thompson, D. P. *J. Eur. Ceram. Soc.* **1994**, *14*, 13.
(4) Jack, K. H. *Processing of Crystalline Ceramics*, Palmour III, H.; Davis, R. F.; Hane, T. M., Eds.; Plenum Press: New York, 1978; p 561.
(5) Slasor, S.; Liddell, K.; Thompson, D. P. *Special Ceramics 8*; Howlett, S. P., Taylor, D., Eds.; The Institute of Ceramics: Shelton, Staffordshire, U.K., 1986; p 51.

0897-4756/95/2807-0982$09.00/0

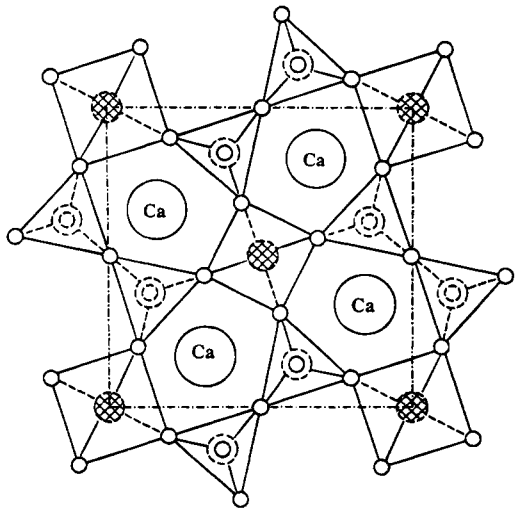

Figure 2. Structure of akermanite showing the MgO_4 sites (corner and center tetrahedra).

NMR experiments, changes in the covalency of the bonds in a structure will lead to different degrees of deshielding of the observed nucleus, causing a change in the resonance frequency, termed the chemical shift. Hence NMR is sensitive to the local environment of the nucleus.[8] The isotropic chemical shift for ^{27}Al can resolve the shift ranges of AlO_4 and AlO_6 units.[9,10] A decrease in the O:N ratio coordinated to a nucleus (i.e., more nitrogen) results in the chemical shift of both ^{27}Al and ^{29}Si resonances shifting to higher frequencies.[6] For ^{29}Si in oxynitride ceramics, it is usually possible to deduce the coordination, SiO_xN_{4-x} ($0 \le x \le 4$), from the ^{29}Si isotropic chemical shift value although there is some overlap of the shift ranges.[8] While local structural information from X-ray diffraction (XRD) in sialon ceramics is limited due to the similar scattering factors of Al and Si, solid-state NMR can provide coordination information. In the present study ^{27}Al and ^{29}Si MAS NMR are used to study their local coordination in a series of yttrium M'_{ss} samples. It is shown that the results are consistent with the prediction that aluminum exclusively occupies the MgO_4 position of the akermanite structure.

Experimental Details

Samples with composition $Y_2Si_{3-x}Al_xO_{3+x}N_{4-x}$ (x = 0.0, 0.1, 0.2, 0.4, 0.6, 0.8, 1.0, and 1.4) were prepared from powders of Y_2O_3 (CERAC), Si_3N_4 (Starck Berlin LC10), AlN (Starck Berlin Grade C), and Al_2O_3 (Unilab). The surface oxide on both "Si_3N_4" and "AlN" was compensated using the calculated formulas of $Si_{2.823}N_{3.645}O_{0.177}$ for "Si_3N_4" and $Al_{1.014}N_{0.985}O_{0.043}$ for "AlN", which allow 4.0 wt % of SiO_2 for the Si_3N_4 powders and 3.5 wt % Al_2O_3 for the AlN powders. The pelletized powder mixes weighing approximately 3 g were placed in a BN-coated graphite crucible and sintered in an induction heating furnace in flowing nitrogen gas at 1600 °C for 2 h. Weight loss of the samples after firing was less than 3%.

The density of the sintered samples was determined by Archimedes principle using a water immersion technique and all samples were boiled in water for 1 h prior to measurement.[11] The major crystalline phases were determined from powder X-ray diffraction (XRD) using a Rigaku Geigerflex diffractometer using Cu Kα radiation of wavelength 0.1541 nm scanning a range of approximately 10−70° 2θ. Additionally the sintered products were characterized by electron microscopy using a JEOL JSM-840A scanning electron microscope (SEM) operating at 20 kV in backscattered mode. Elemental analysis was performed using energy-dispersive X-ray spectra (EDXS) obtained from a spectrometer attachment on the SEM. The bulk samples were polished and carbon coated to prevent surface charging in the electron beam.

MAS NMR analysis was performed on a Bruker MSL-400 spectrometer operating at 104.23 MHz for ^{27}Al and 79.47 MHz for ^{29}Si. The powdered samples were packed into conventional zirconia spinners and were spun at 12 and 4.5 kHz for ^{27}Al and ^{29}Si respectively. ^{29}Si NMR spectra were accumulated using 1.5 μs (tip angle ~30°) pulses with 15 s recycle delays which, in view of the long spin−lattice relaxation times for ^{29}Si, may result in spectra that are not fully relaxed but allowed adequate signal-to-noise to be obtained. The corresponding conditions for ^{27}Al were 0.65 μs (15°) pulses, a preacquisition delay of only 5 μs and a 1−2 s recycle delay that produced fully relaxed spectra. To determine the contributions to the ^{27}Al line width, some additional spectra were acquired at 156.32 MHz on a Varian VXR-600 spectrometer with other acquisition conditions similar to those described at 104.23 MHz. ^{27}Al spectra were referenced against an external secondary standard of $Y_3Al_5O_{12}$ (AlO_6 = 0.7 ppm with respect to $[Al(H_2O)_6]^{3+}$). ^{29}Si MAS NMR spectra were referenced to tetramethylsilane (TMS) at 0 ppm.

An important question for all ^{27}Al NMR spectra from solids is to establish the quantitative integrity of these NMR spectra. As a result of early ^{27}Al MAS NMR results, it is often thought that only a small fraction of the total aluminum may be contributing to the observable signal. However in recent years improvements in spectrometer hardware, in particular much faster recovery of the probes and receiver system, the use of short, small tip angle pulses and using very fast digitization rates means that even very broad unnarrowed spectral components are now observable. The faster MAS now available (12 compared to 5 kHz) is also a big advantage. High quantitative accuracy in MAS NMR spectra is now possible even when large quadrupolar interactions are present, e.g., yttrium aluminum garnet,[12] kyanite,[13] and andalusite.[13] Even in other silicon−aluminum−oxygen−nitrogen (sialon) ceramics where very distorted local aluminum environments can occur, it has been shown that there has been a great improvement in the amount of aluminum observed (compare refs 7 and 14). On the basis of experience, quantification of ^{27}Al NMR spectra of comparable sialon ceramics with the current conditions at 9.4 T > 90% of the aluminum content is observed.

Results and Discussion

Crystalline Phases. Table 1 shows the densities and major crystalline phases present after sintering as determined from XRD. Previous studies have found that with increasing aluminum concentration in the Sm M'_{ss} system it moves toward the liquid-phase region, and consequently a liquid phase then assists densification of the materials.[2] On cooling most of the eutectic liquid crystallizes leaving little glass. In the present work, a significant increase in the density has been observed when Al content increased (from sample Y0 to Y14) consistent with increased liquid-phase sintering promoting more efficient densification.

(6) Dupree, R.; Lewis, M. H.; Smith, M. E. *J. Am. Chem. Soc.* **1989**, *111*, 5125.
(7) Smith, M. E. *J. Phys. Chem.* **1992**, *96*, 1444.
(8) Dupree, R.; Lewis, M. H.; Smith, M. E. *J. Am. Chem. Soc.* **1988**, *110*, 1083.
(9) Hatfield, G. R.; Carduner, K. R. *J. Mater. Sci.* **1989**, *24*, 4209.
(10) Smith, M. E. *Appl. Magn. Reson.* **1993**, *3*, 1.
(11) Kingery, W. D.; Bowen, H. K.; Uhlmann, D. R. *Introduction to Ceramics*; J. Wiley and Sons: New York, 1976; p 530.
(12) Massiot, D.; Bessada, C.; Coutures, J. P.; Taulelle, F. *J. Magn. Reson.* **1990**, *90*, 231.
(13) Alemany, L. B.; Massiot, D.; Sherriff, B. L.; Smith, M. E.; Taulelle, F. *Chem. Phys. Lett.* **1991**, *177*, 301.
(14) Dupree, R.; Lewis, M. H.; Smith, M. E. *J. Appl. Cryst.* **1988**, *21*, 109.

Table 1. Summary of Overall Composition, Density, and XRD Results[a]

sample	overall composition	density (g cm^{-3})	crystalline phases as determined by XRD			
Y0	$Y_2Si_3O_3N_4$	3.177	M(s)	J(ms)	β-Si_3N_4(mw)	
Y1	$Y_2Si_{2.9}Al_{0.1}O_{3.1}N_{3.9}$	3.476	M′ss(vs)	J′ss(m)	β-Si_3N_4(w)	
Y2	$Y_2Si_{2.8}Al_{0.2}O_{3.2}N_{3.8}$	3.455	M′ss(s)	J′ss(m)		
Y4	$Y_2Si_{2.6}Al_{0.4}O_{3.4}N_{3.6}$	3.623	M′ss(s)	J′ss(ms)	Woll(m)	α-Si_3N_4(w)
Y6	$Y_2Si_{2.4}Al_{0.6}O_{3.6}N_{3.4}$	4.048	M′ss(vs)	J′ss(mw)		
Y8	$Y_2Si_{2.2}Al_{0.8}O_{3.8}N_{3.2}$	3.889	M′ss(vs)	J′ss(m)	YAG(mw)	α-Si_3N_4(w)
Y10	$Y_2Si_{2.0}Al_{1.0}O_{4.0}N_{3.0}$	3.914	M′ss(s)	J′ss(vs)	YAG(m)	α-Si_3N_4(vw)
Y14	$Y_2Si_{1.6}Al_{1.4}O_{4.4}N_{2.6}$	3.947	M′ss(ms)	J′ss(vs)	21R(m)	

[a] M = N-melilite,$Y_2Si_3O_3N_4$; M′ss = Al-containing N-melilite $Y_2Si_{3-x}Al_xO_{3+x}N_{4-x}$; J = $Y_4Si_2O_7N_2$; J′ss = $Y_4Si_{3-x}Al_xO_{7+x}N_{2-x}$; Woll = $YSiO_2N$; YAG = $Y_3Al_5O_{12}$; 21R = $SiAl_6O_2N_6$. X-ray intensities: s = strong, m = medium, w = weak, v = very.

N-melilite is detected as the major phase in the Al-free sample (Y0) by XRD. As Al is introduced into the system, the basic XRD pattern of the N-melilite phase is maintained in all the samples but a clear increase in the *d* spacing calculated from XRD profile of the phase is observed,[15] suggesting formation of aluminum-containing melilite solid solution (M'_{ss})[2]. Unlike the samarium and neodymium systems in which formation of M'_{ss} is relatively easy,[2,16] single-phase yttrium M'_{ss} proved difficult to produce and the samples always contained a number of phases. Traces of unreacted Si_3N_4 were found in some of the fired samples as a relatively low sintering temperature was employed to ensure low weight loss. The main impurity phase is the oxygen-rich solid solution between $Y_4Si_2O_7N_2$ (J phase) and $Y_4Al_2O_9$ (YAM) of composition $Y_4Si_{2-x}Al_xO_{7+x}N_{2-x}$ (J'_{ss}) which forms from the initial reaction between Y_2O_3 and surface SiO_2 present around the Si_3N_4 particles. An SEM micrograph of sample Y6 shows its multiphase nature and the residual porosity (Figure 3). EDXS analysis identified the majority phase as M'_{ss} with some J'_{ss}, in good agreement with the XRD data (Table 1). When the Al content is high, YAG ($Y_3Al_5O_{12}$) was detected in samples Y8 and Y10 and 21R AlN-polytypoid ($SiAl_6O_2N_6$) was found in sample Y14. From these results apparently the final compositions of the samples lie in two of the known equilibrium phase regions in the Y−Si−Al−O−N system,[17] either J'_{ss} + M'_{ss} or J'_{ss} + M'_{ss} + YAG, depending on the aluminum concentration, and are in good agreement with previous studies of phase equilibria in this system.[2,3,17,18]

^{27}Al MAS NMR Spectra. Figure 4 shows the ^{27}Al MAS NMR spectra of the melilite-containing samples. Due to the multiphase products, the spectra are somewhat complex. Apart from spinning sidebands in samples Y8 and Y10, there are four readily distinguishable peaks in most of the spectra, namely, peaks A−D. A more positive peak position indicates a decrease in the shielding by the coordinating groups, caused by a reduction in coordination number or by nitrogen replacing oxygen as a nearest neighbor (nn). These fully relaxed spectra would allow the quantitative phase distribution to be deduced, but the large degree of overlap of some resonances which are asymmetric makes spectral integration difficult and the spectra are used only qualitatively here. Nevertheless the keypoint is to be able to identify the resonances associated with M'_{ss}.

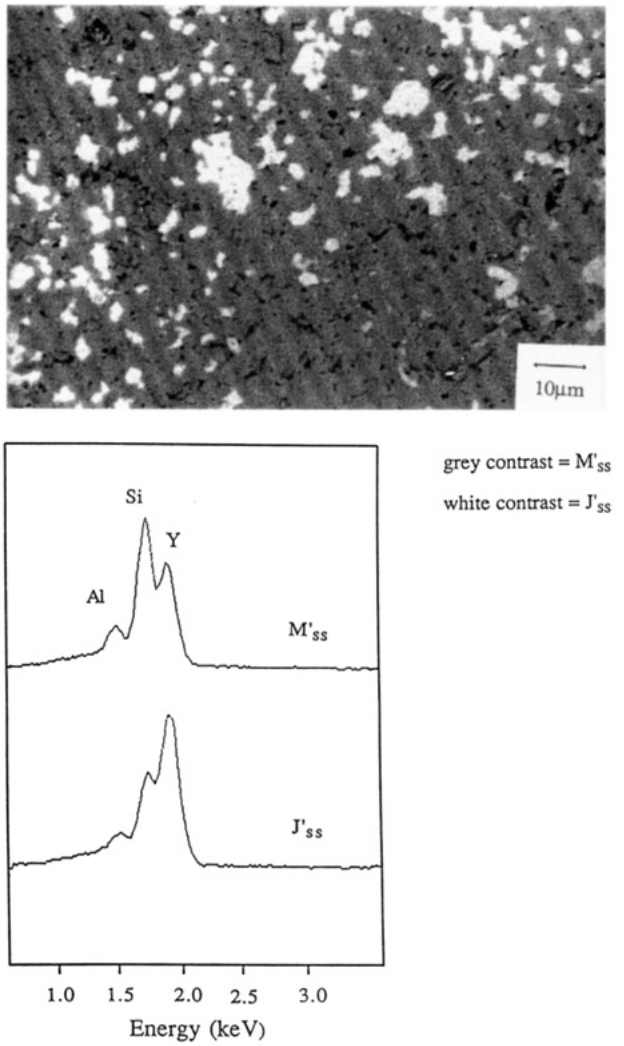

Figure 3. Backscattered SEM image and EDXS analysis of sample Y6. In the micrograph white regions correspond to J'_{ss} ($Y_4Si_{2-x}Al_xO_{7+x}N_{2-x}$) in the gray matrix of M'_{ss}($Y_2Si_{3-x}Al_xO_{3+x}N_{4-x}$) with the pores appearing as black regions.

It is also important to realize that Al (nuclear spin $I = 5/2$) possesses a nuclear electric quadrupole moment. The quadrupolar interaction can complicate interpretation of MAS NMR spectra since if this interaction is large enough, second-order effects have to be considered.[10] MAS can only partially remove second-order broadening and the peak position does not correspond to the isotropic chemical shift and is a function of applied magnetic field. As the second-order quadrupolar interaction leaves a residual width in MAS spectra

(15) Chee, K. S.; Cheng, Y-B.; Smith, M. E.; Bastow, T. J. *Proc. Austceram 94*; Sorrell, C. C., Ruys, A. J., Eds.; Australasian Ceramic Society: Sydney, Australia, 1994; p 1031.
(16) Chee, K. S.; Cheng, Y.-B.; Smith, M. E., manuscript in preparation.
(17) Sun, W.-Y.; Huang, Z.-K; Cheng, J.-X. *Trans. Br. Ceram. Soc.* **1983**, *82*, 173.
(18) Sun, W.-Y.; Yan, D.-S.; Tian, Z.-Y. *Sci. China (Ser. A)* **1992**, *35*, 877.

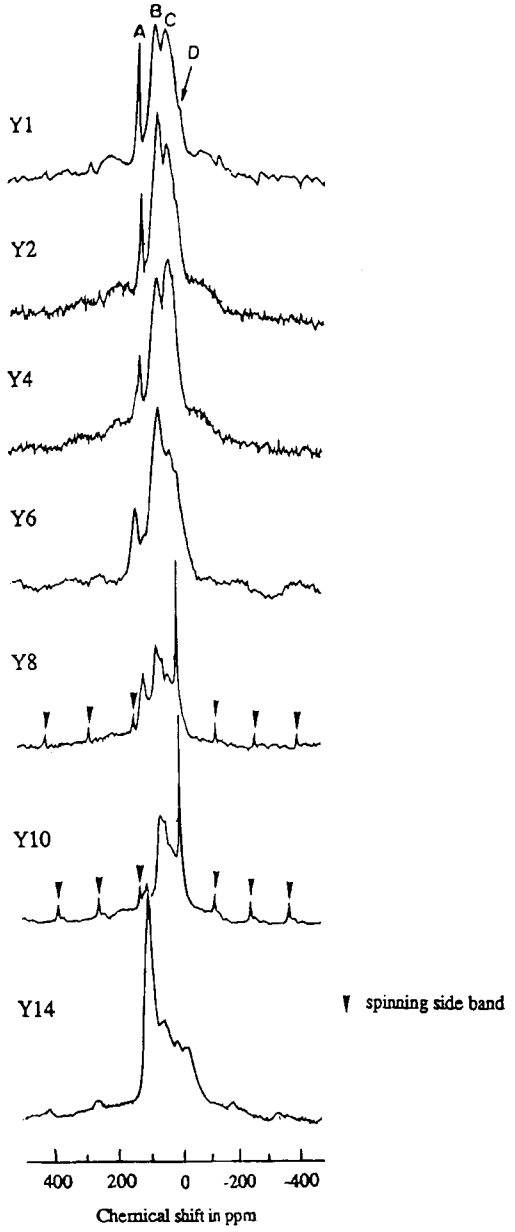

Figure 4. ^{27}Al MAS NMR spectra at 9.4 T of M′$_{ss}$-containing samples following the designation of Table 1.

to ensure that as large as possible quadrupolar interaction is narrowed to some extent under MAS the fastest available MAS should be used. In most ceramic materials, to a first approximation ^{27}Al MAS NMR spectra have two major contributions to the line width, residual second-order quadrupolar broadening ($\Delta\nu_Q$ in Hz T^{-1}) and dispersion of the chemical shift $\Delta\nu_{cs}$, so that the total line width in Hz at an applied field B_0 is given by

$$\Delta\nu = \Delta\nu_Q B_0^{-1} + \Delta\nu_{cs} B_0 \qquad (1)$$

Hence, line width can vary from directly to inversely proportional to B_0 depending on which term is dominant. Disorder that causes a spread of quadrupolar coupling constants results in the line becoming asymmetric with a tail to negative shift, complicating spectral deconvolution.[19]

Peak A in Figure 4 with a peak position of ~110 ppm is typically associated with AlN_4 units. In samples Y1 to Y8, this peak is attributed to residual AlN from the original powder mixture. The presence of AlN was not detected by XRD, but this is not unexpected since the concentration of AlN in the samples is very low as indicated by the relatively small area under peak A (~2%). This narrow peak is indicative of a relatively ordered crystalline phase. It does not show up in the XRD pattern since this pattern is dominated by the crystalline compounds containing heavy elements (here yttrium) due to the proportionality of the X-ray scattering factor to atomic number. The amplitude of this peak decreases from Y1 to Y8 and is consistent with the fact that as more Al is added to the system, more liquid forms that increases the reaction rate of AlN. When Al addition is high such as in Y14, a strong, broad peak near A appears and this is attributed to AlN_4 in 21R AlN–polytypoid.[7]

Peak C at ~30 ppm is not common for ^{27}Al MAS NMR in Si–Al–O–N systems.[6,7] In crystalline aluminosilicates well-defined AlO_5 units are rare, but those measured indicate isotropic chemical shifts of between 30 and 40 ppm (summarized in Table 1 in ref 20). Similarly AlO_5 resonances have also been observed in aluminosilicate glasses,[21] thermal decomposition of aluminosilicate minerals,[22] and amorphous aluminas.[23] The peaks from these sites tend to appear in the range 35–25 ppm with some field dependence from the residual second-order quadrupolar shift. Narrow peaks in the ^{29}Si MAS NMR spectra (vide infra) indicate that there is only limited glass present in the system and is unlikely to account for the high intensity of peak C. Although the ^{29}Si MAS NMR spectrum of J′$_{ss}$ phase has been reported,[6] information on the ^{27}Al MAS NMR resonance of this phase is very limited. To obtain more information, a J′$_{ss}$ phase with composition Y_4SiAlO_8N was prepared and sintered at 1600 °C for 2 h and characterized by XRD. The XRD trace shows almost single phase J′$_{ss}$ with a trace amount of 21R AlN-polytypoid after sintering (Figure 5a) as expected from phase relationships in the Y–Si–Al–O–N system.[18] The dominant peak in the ^{27}Al MAS NMR spectrum at 9.4 T of the J′$_{ss}$ phase (Figure 5b) has a peak position of ca. 30 ppm. The J′$_{ss}$ phase did not form in samarium M′$_{ss}$-containing samples,[2,15] and as a result the 30 ppm peak disappeared from the ^{27}Al MAS NMR spectra of the samarium system, providing further evidence for the above argument. The resonance at ~110 ppm in Figure 5b comes from the AlN_4 unit in AlN or 21R AlN-polytypoid.

Work at 156.2 MHz compared the ^{27}Al NMR spectra from a J′$_{ss}$ sample (Figure 6a) and that from Y1 (Figure 6b). The comparative change in these two spectra in going from 9.4 to 14.1 T is very striking. The J′$_{ss}$ sample shows much better resolution at the higher field as a result of the three main peaks at 110, 60, and 30 ppm all being narrower. The implication is that second-order quadrupole effects must be determining the line width

(19) Jaeger, C.; Kunath, G.; Losso, P.; Scheler, G. *Solid State NMR* **1993**, *2*, 73.
(20) Smith, M. E.; Steuernagel, S. *Solid State NMR* **1992**, *1*, 175.
(21) Sato, R. K.; McMillan, P. F.; Dennison, P.; Dupree, R. *J. Phys. Chem.* **1991**, *95*, 4483.
(22) Smith, M. E.; Neal, G.; Trigg, M. B.; Drennan, J. *Appl. Magn. Reson.* **1993**, *4*, 157.
(23) Farnan, I.; Dupree, R.; Forty, A. J.; Yeong, Y. S.; Thompson, G. E.; Wood, G.C. *Philos. Mag. Lett.* **1989**, *59*, 189.

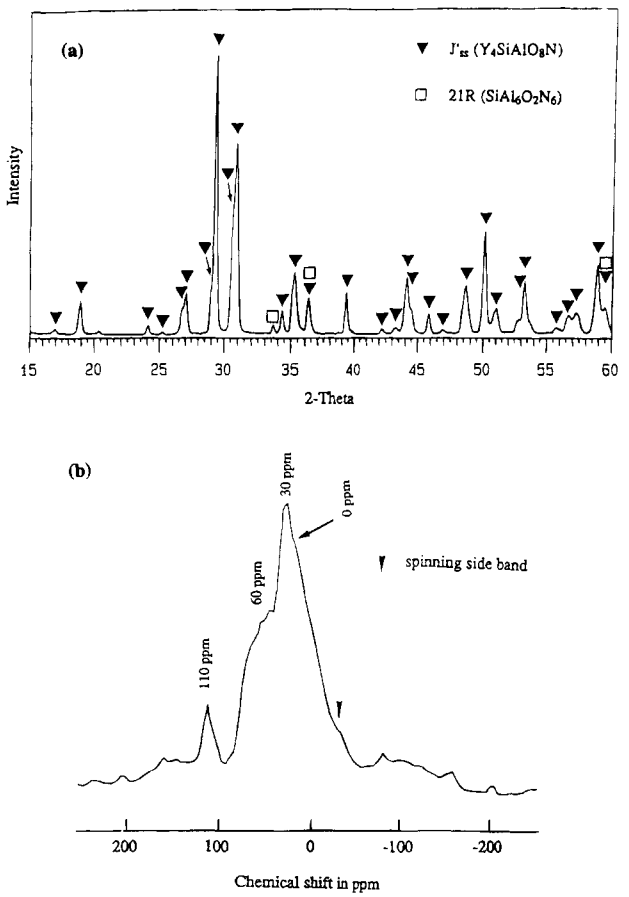

Figure 5. (a) XRD and (b) ^{27}Al MAS NMR spectra at 9.4 T of J'_{ss} (Y_4SiAlO_8N).

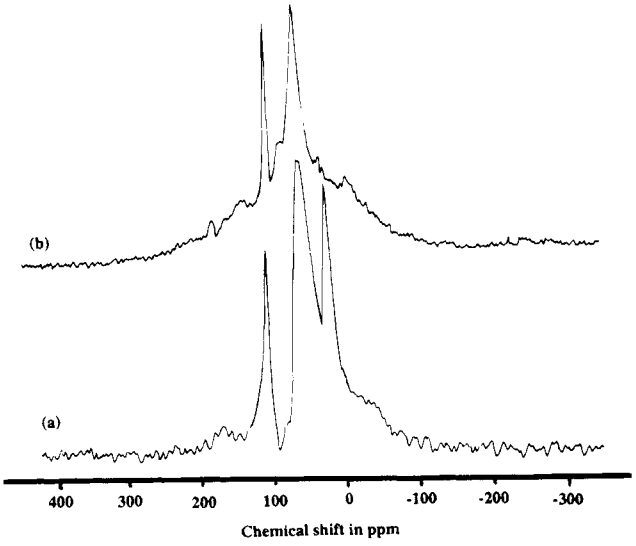

Figure 6. ^{27}Al MAS NMR spectra at 14.1 T of (a) Y_4SiAlO_8N and (b) M'_{ss} (Y1) sample.

(eq 1) in this sample, so that the sample is crystalline and atomically well ordered. The structural explanation of the 30 ppm peak in J'_{ss} is at present unclear and is part of a current investigation. For M'_{ss} peaks A and B at ~110 and 65 ppm are narrower at 14.1 T than at 9.4 T but at the higher field the 30 ppm peak is no longer apparent. The explanation of this observation is that the 30 ppm peak in Y1 has a large chemical shift dispersion contribution to the line width. This contribution scales proportionally with the magnetic field (in hertz) so that the spinning rates available at 14.1 T are not able to narrow this increased width and results in the intensity from this (and other sites) as an observable broad underlying peak (Figure 6b). Hence in Y1 the AlO_4 and AlO_5 peaks must come from different phases, with the former better ordered. The AlO_5 peak in Y1 is either an amorphous phase or an atomically disordered aluminum-rich J'_{ss} phase. This spectrum also shows that the aluminum-content of the M'_{ss} is below the nominal target (0.1), but nevertheless the clear implication of the observed spectrum is that the aluminum that **has** dissolved in N-melilite in Y1 is clearly a well-defined AlO_4 group. This illustrates how important multiple magnetic field studies are for obtaining maximum information about ^{27}Al resonances.

Peak D is from AlO_6 in some very minor phase, such as a polytypoid or more likely, an alumina or other yttrium aluminate phase (Figure 4). It can also be seen as a minor peak in the 14.1 T data of Y1 (Figure 6b). Peak D appears to increase in intensity from sample Y1 to Y6, consistent with an increase in the alumina content but nevertheless remains a very minor phase. In samples Y8 and Y10, peak D is narrow and more prominent due to the strong AlO_6 resonance in YAG.[12,14] The sharp peak D disappears in sample Y14 which does not contain YAG and is replaced by a broad peak D which is associated with the AlO_6 structural unit in 21R AlN−polytypoid.[7] Both YAG and 21R were detected by XRD in the respective samples.

The strongest ^{27}Al resonance for most of the samples appears at ~60 ppm (peak B) which is normally associated with AlO_4 in Si−Al−O−N compounds.[7] Although a small portion of this peak may be attributed to AlO_4 from J'_{ss}, consideration of the nature of ^{27}Al MAS NMR resonances and the different shape and field dependence of the AlO_4 resonance observed in the M'_{ss} sample and J'_{ss}, together with the known structure of N-melilite indicate that peak B is from the Al environment in M'_{ss}. It is known that N-melilite consists of tetrahedral sheets and that all the Si atoms are arranged in an SiO_2N_2 tetrahedral coordination in the structure.[8] In Al-free N-melilite, there is no four nitrogen-coordinated Si, and it is even less likely for Al to be present as AlN_4 in the solid solution structure because the replacement of Al for Si involves the concomitant substitution of O for N atoms. On the other hand, if a mixed Al coordination of the type $AlO_{4-x}N_x$ ($0 < x < 4$) formed, it would result in a peak, or peaks, present in the range between ~60 ppm (for AlO_4) and ~110 ppm (for AlN_4);[7] however, this was not observed in the ^{27}Al MAS NMR spectra in Figures 4 or 6b. The position of peak B is unaltered by the extent of Al substitution, and no other peaks appear in the range 60−110 ppm that cannot be explained by other phases, indicating a constant coordination for Al in M'_{ss}. Therefore, it is concluded that in the M'_{ss} phase, Al has a unique coordination with four oxygen atoms that does not change with composition. It should be pointed out that the "splitting" of peak B in samples Y8 and Y10 is due to the AlO_4 resonance in YAG superimposed on that from M'_{ss}.[12,14]

^{29}Si MAS NMR Spectra. Figure 7 shows the ^{29}Si MAS NMR spectra of the same series of M'_{ss}-containing samples. In ^{29}Si MAS NMR spectra there is a trend toward positive chemical shifts with increasing replacement of Si−N bonds for Si−O bonds.[6] In sialon ceramics, Si is always four-coordinated, and previous work has

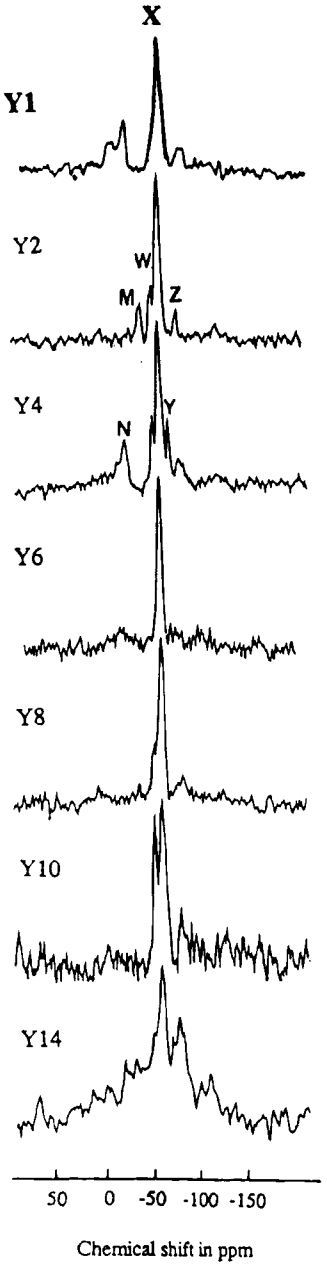

Figure 7. ^{29}Si MAS NMR spectra at 9.4 T of M'_{ss}-containing samples following the designation of Table 1.

been able to demonstrate the relationship between chemical shift and the oxygen-to-nitrogen ratio in SiO_xN_{4-x} ($0 \le x \le 4$) tetrahedra for phases in the Y–Si–O–N system.[8] By referring to those chemical shifts, the multiple ^{29}Si MAS NMR resonances obtained here can be unambiguously assigned to phases determined by XRD. The recycle times used here for ^{29}Si were chosen to maximise the signal-to-noise.[24] Under the conditions used here it is probable that the ^{29}Si MAS NMR spectra will record all phases but overestimate the content of some of those phases due to the large variation of relaxation times. This is exemplified by peak W in sample Y10 (Figure 7) where the actual concentration of residual Si_3N_4 is not as high as indicated by the amplitude. Also the minor peaks in Y1 at around −20 and −75 ppm largely disappeared in an experiment where a single pulse was acquired after leaving 15 h for magnetization equilibration. However, the spectra do allow ready identification of all the phases present.

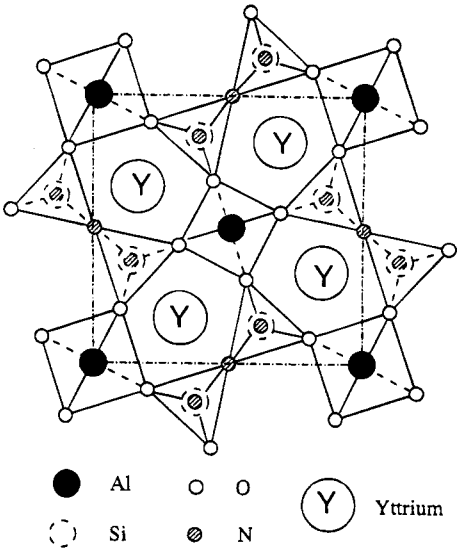

Figure 8. Proposed atomic arrangement of M'_{ss} at the composition $Y_2Si_2AlO_4N_3$ (i.e., maximum aluminum solubility) consistent with the NMR results.

For the majority of the samples, the most positively shifted peak in the spectra is peak W (−48 ppm) and this peak is associated with the SiN_4 unit from traces of unreacted Si_3N_4. Peak Y (−64 ppm) is only observed in sample Y4 and is due to SiO_2N_2 from wollastonite ($YSiO_2N$) as confirmed by XRD results (Table 1) and Peak Z (−75 ppm) is detected in most of the samples from the SiO_3N coordination in J'_{ss}.[8] Samples Y2 and Y1, Y4 have additional resonances, peak M (−40 ppm) and peak N (−20 ppm), respectively, which are not present in the other samples. While these impurities were not detected from XRD due to the complex diffraction patterns arising from the multiphase samples, the chemical shift of peak M correlates with the ^{29}Si MAS NMR resonance for YSi_3N_5, observed as an initial phase during the preparation of Al-free N-melilite.[8] The ^{29}Si MAS NMR resonance at ∼−20 ppm has to date never been observed for phases in the Y–Si–Al–O–N system and is probably due to a SiC polytype impurity[9] which formed from the reaction between the graphite crucible and SiO vapor. A peak at −20 ppm has previously been observed in the initial stages of sialon formation by carbothermal reduction of clay minerals by this very reaction mechanism and is very sensitive to the local partial pressure of the various gaseous species present.[25] Peak X at ∼−57 ppm is attributable to SiO_2N_2 observed in $Y_2Si_3O_3N_4$.[8] This peak is observable throughout this series of compounds indicating that the Si environment in N-melilite is unaltered by Al substitution.

Proposed Structure of Yttrium M'_{ss}. The above XRD results have shown that M'_{ss} possesses the same crystal structure as Al-free N-melilite. In the M'_{ss} structure, Al appears coordinated as AlO_4 throughout the solubility range and Si is coordinated as SiO_2N_2, forming the tetrahedral sheet in the M'_{ss} structure. To accommodate the structural units assigned to the M'_{ss} phase, Figure 8 depicts the proposed schematic atomic arrangement of yttrium M'_{ss} projected on the (001)

(24) Dupree, R.; Smith, M. E. *J. Magn. Reson.* **1987**, *75*, 153.

(25) Neal, G. S.; Smith, M. E.; Trigg, M. B.; Drennan, J. *J. Mater. Chem.* **1994**, 4, 245.

plane. The Al atoms are situated in the corner and center positions of the unit cell coordinated as AlO_4, and these tetrahedra are linked by double tetrahedral groups consisting of two SiO_2N_2 units to form a continuous sheet structure. The yttrium atoms are located between these sheets. This type of structure suggests a terminal composition of $R_2Si_2AlO_4N_3$ (R = Y and rare-earth elements) for aluminum-containing N-melilite phases. This deduction is supported by results obtained in samarium and neodymium M'_{ss} systems.[2,16]

Excess Al substitution beyond $x = 1.0$ would result in Al atoms entering the double $[Si_2(O,N)_7]$ tetrahedral groups. In the original akermanite structure the cation–oxygen distance in the $[Si_2O_7]$ double tetrahedra (1.63 Å) is much smaller compared to that in the tetrahedra at the corners (1.87 Å);[26] therefore incorporation of Al (Al–O bond length = 1.75 Å) into the $[Si_2(O,N)_7]$ group could generate a large amount of stress in the lattice and destabilize the structure. Furthermore, this would produce two inequivalent Al sites in the M'_{ss} structure AlO_4 and AlO_3N which should give a distinguishable resonance in the ^{27}Al MAS NMR spectra between ~60 ppm (for AlO_4) and ~110 ppm (for AlN_4) from the mixed anion environment. Such a resonance is not observed in the current NMR data. While the maximum theoretical Al solubility that can be achieved with this kind of atomic arrangement is $x = 1.0$, the actual solubility in different M'_{ss} systems could be lower depending on other considerations of crystal chemistry and thermodynamics. It has been noted that the size of cation that holds the tetrahedral sheets together has a significant effect on the solubility of Al in the M'_{ss} structure.[15] Moreover it is suggested that when the Al content is less than maximum, so that only some of the available Al sites are occupied as AlO_4 units, the other corner and center tetrahedra would then be SiO_2N_2. This conclusion arises from the fact that chemical shifts for both Al and Si nuclei are independent of the extent of Al solubility in the M'_{ss} structure.

(26) Smith, J. V. *Am. Mineral.* **1953**, 38, 643.

Conclusions

A possible atomic arrangement of yttrium M'_{ss} that is consistent with the local environments determined from ^{27}Al and ^{29}Si MAS NMR has been proposed. The incorporation of Al does not change the original structure of N-melilite, but the continuous tetrahedral sheet in M'_{ss} has been found to consist of both AlO_4 and SiO_2N_2 units. There is no evidence of a change in the coordination of Al as the composition varies. All the NMR evidence is consistent with aluminum occupying corner and center sites of the layers (i.e., the MgO_4 sites in the analogous akermanite structure) resulting in the maximum Al solubility in M'_{ss} being $x = 1.0$ (i.e., $Y_2Si_2AlO_4N_3$). This illustrates that even in complex phase mixtures NMR can be very helpful for interpreting other observations in terms of atomic scale structure.

Acknowledgment. The authors wish to thank Dr. T. J. Bastow from CSIRO Division of Materials Science and Technology for performing some of the NMR experiments. CSIRO is thanked for partial support and MES thanks the EPSRC for access to the ultrahigh field NMR facility at the University of Edinburgh and Dr. J. Parkinson for his help there.

CM940561N